



Cite this: *RSC Adv.*, 2017, 7, 15762

# Preparation and characterization of a novel imidacloprid microcapsule *via* coating of polydopamine and polyurea†

Zideng Gao,<sup>a</sup> Long Pang,<sup>a</sup> Haojie Feng,<sup>a</sup> Shunyi Wang,<sup>a</sup> Qiuyun Wang,<sup>a</sup> Mengyao Wang,<sup>a</sup> Yining Xia<sup>\*b</sup> and Shuwen Hu<sup>\*a</sup>

Encapsulation of pesticides with polymeric materials is a promising approach to improve the efficacy of pesticide application and reduce the potential risks of pesticides to the environment and humans. In this study, a novel imidacloprid microcapsule was prepared by depositing a polydopamine (PDA) layer on imidacloprid *via* oxidative self-polymerization followed by a polyurea (PU) layer on PDA *via* copolymerization. No organic solvent or surfactant was used in the preparation process. The entrapment rate of imidacloprid was determined to be  $47.28 \pm 0.87\%$ , and the pesticide loading of microcapsule was  $68.36 \pm 1.13\%$ . Several characterization assays, such as Fourier infrared transform analysis, thermogravimetric analysis and contact angle analysis, were conducted to confirm the encapsulation of imidacloprid. Dynamic light scattering showed that the microcapsule size ranged from hundreds of nm to several  $\mu\text{m}$ , which was similar to the results obtained by scanning electron microscopy. The microcapsule had a stable dispersion up to one month in the aqueous solution. Moreover, the microcapsule was able to release imidacloprid in a sustainable manner, as the release was much slower than the non-encapsulated imidacloprid.

Received 6th February 2017  
Accepted 6th March 2017

DOI: 10.1039/c7ra01527e

rsc.li/rsc-advances

## 1. Introduction

Imidacloprid 1-(6-chloro-3-pyridinylmethyl)-*N*-nitro-2-imidazolidinimine is a neonicotinoid insecticide having outstanding potency and systemic action for crop protection against piercing-sucking pests.<sup>1</sup> It has dominated the global insecticide market with advantages of high specificity, high efficiency and low toxicity to non-target organism.<sup>2,3</sup> Since first introduction in 1991 by Bayer CropScience, products containing imidacloprid have gained registrations for over 140 crops in more than 120 countries.<sup>4</sup> Nevertheless, the wide use of imidacloprid causes adverse effects such as soil pollution,<sup>5</sup> surface/underground water contamination,<sup>6</sup> destructions of biological systems<sup>5</sup> and damages to human health.<sup>7</sup> These problems can be reduced *via* controlled release formulations (CRFs) prepared through green process.

Microcapsule-controlled release technology has been widely applied in the fields of pharmaceuticals, biotechnology,

pesticides, environmental engineering, cosmetics, coatings and food chemistry, offering an ideal solution to the efficient delivery of target molecules.<sup>8,9</sup> In the field of pesticides, pesticide microcapsule formulations for controlled release bring several advantages over the conventional formulations, such as protecting pesticides from rapid environmental wastage, increasing the performance level of pesticides efficiently, and reducing potential risks to the environment and humans.<sup>10</sup>

Pesticide microcapsule formulations can be prepared by encapsulation of pesticides *via* different routes, including interfacial polymerization,<sup>11,12</sup> *in situ* polymerization<sup>13</sup> and condensation,<sup>14</sup> and solvent evaporation.<sup>15,16</sup> However, the preparation of imidacloprid microcapsule formulations is difficult due to the poor solubility of imidacloprid in common solvents at room temperature (*e.g.*,  $0.61 \text{ g L}^{-1}$  in water,  $50 \text{ g L}^{-1}$  in 2-butanone).<sup>17,18</sup> A few studies have successfully obtained the imidacloprid microcapsules in an aqueous solution by preparing a water-insoluble imidacloprid-encapsulating matrix and coating the matrix *via* interfacial polymerization.<sup>19-21</sup> In these studies, a variety of surfactants were applied to maintain stable interfaces (*e.g.*, water/oil, solid/water and solid/oil) in the encapsulating system. The use of surfactants improved the microparticle dispersion in the aqueous solution, while they can easily interfere with each other during the preparation process and cause environmental problems after applied to farmland.<sup>22,23</sup> In addition, the high shear forces applied to produce very small droplets may cause break down of the

<sup>a</sup>College of Resources and Environmental Sciences, China Agricultural University, Beijing 100193, China. E-mail: shuwenhu@cau.edu.cn; Fax: +86 010 62731016; Tel: +86 010 62731255

<sup>b</sup>Institute of Quality Standard and Testing Technology for Agro-Products, Chinese Academy of Agricultural Sciences, Beijing 100081, China. E-mail: xiayingning@caas.cn; Tel: +86 010 82106358

† Electronic supplementary information (ESI) available. See DOI: 10.1039/c7ra01527e



encapsulating matrix and then release of pesticide from the encapsulating matrix. Therefore, many efforts need to be carried out to create more reliable and sustainable imidacloprid microcapsule systems.

Dopamine (3,4-dihydroxyphenethylamine), which contains a catechol group and an amine group, can be simply deposited on a surface to form a layer through oxidative self-polymerization.<sup>24,25</sup> The polydopamine (PDA) layer contains multiple functional groups (amino, imino and catechol groups) that can be used for secondary reactions.<sup>24–26</sup> Recently, PDA has received increasing interest in the fields of surface chemistry, material and membrane science.<sup>27</sup> The main applications include drug delivery and controlled release,<sup>28</sup> surface modification of a material<sup>29,30</sup> and coating of insoluble microparticles.<sup>31,32</sup> PDA is considered a promising candidate for the encapsulation of imidacloprid to obtain imidacloprid microcapsules.

This study aimed to develop a novel imidacloprid microcapsule with the use of dopamine and diisocyanate to achieve stable dispersion and sustained release in water. Three types of imidacloprid formulations (IMFs), imidacloprid suspension (IMSC), polydopamine coated imidacloprid (IMPDA) and polyurea coated IMPDA (IMPU), were prepared step by step. No surfactant or organic solvent was used during the preparation process. In the first step, IMSC was obtained by a wet grinding process. In the second step, IMSC was obtained by a wet grinding process. In the second step, dopamine was used to form a layer by oxidative self-polymerization on the surface of IMSC. The resulting product (known as IMPDA) was rich in amino and hydroxyl groups on the PDA layer, making it easy to disperse in water and react with diisocyanate. In the last step, IMPDA was prepared by polymerization of isophorone diisocyanate (IPDI) on the PDA layer of IMPDA. The prepared imidacloprid microcapsules were characterized on physicochemical properties including thermal properties, size and size distribution, morphology, hydrophilicity and dispersion stability. The entrapment rate and pesticide loading as well as the sustained release properties were also investigated.

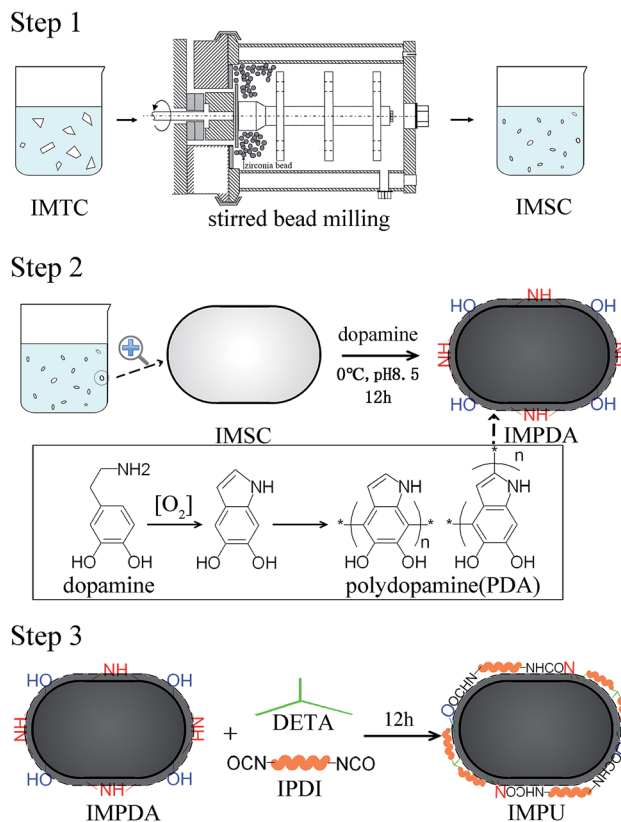
## 2. Experimental

### 2.1 Materials

The chemical reagents used were diethylenetriamine (DETA, chemical pure, National Medicine Group Chemical Reagent Co., Ltd, Beijing, China), isophorone diisocyanate (IPDI, 99%, J&K Beijing Science and Technology Co., Ltd, Beijing, China), dopamine hydrochloride (98%, Shanghai Aladdin Reagent Co Ltd, Shanghai, China), imidacloprid (96.6% TC, Jiangsu Aijin Agrochemical Co., Ltd., Nanjing, China), dibutyl sebacate (DBS, chemical pure, National Medicine Group Chemical Reagent Co., Ltd, Beijing, China), triethanolamine (TEA, chemical pure, National Medicine Group Chemical Reagent Co., Ltd, Beijing, China), and Tris/HCl buffer (1 M, pH = 8.5, Beijing Leagene Biotechnology Co., Ltd, Beijing, China).

### 2.2 Preparation of imidacloprid microcapsules

Imidacloprid microcapsules were prepared in three steps (Scheme 1). Optimization of the preparation conditions was



Scheme 1 Schematic for the preparation process of IMFs (IMSC, IMPDA and IMPU).

conducted and described in the ESI.† Eventually, the optimized preparation conditions were selected to prepare imidacloprid microcapsules. In the first step, imidacloprid TC (20 g) and deionized water (300 mL) was added into a 500 mL flask equipped with a mechanical stirring and stirred at 800 rpm for 10 min to prepare the preliminary suspension. The suspension was then transferred to a stirred bead milling (0.8–1.2 mm zirconia bead, STWZX-0.4-II, Shanghai SuoTn Mechanical & Electrical Equipment Co., Ltd), and wet ground at 2000 rpm for 2 h to obtain IMSC. In the second step, IMSC (20 mL), dopamine hydrochloride (40 mg) and Tris/HCl buffer (200 μL, pH = 8.5) were added into a 50 mL flask, and magnetically stirred (300 rpm, 12 h) in an ice water bath to obtain IMPDA.<sup>24</sup> In the last step, DETA (110 μL) as a cross linker was directly added into the IMPDA suspension prepared in the second step and stirred at 300 rpm for 2 h. After that, IPDI (220 μL) was slowly added into the suspension and stirred at 2000 rpm for 10 min and then at 500 rpm for 12 h to obtain IMPU. The suspensions of IMPDA and IMPU was centrifuged (12 000 rpm, 5 min), washed with water for at least three times, and freeze-drying to obtained IMPDA and IMPU microcapsules.

### 2.3 Characterization of imidacloprid microcapsules

**2.3.1 Entrapment rate and pesticide loading.** The encapsulation efficiency was estimated by entrapment rate (ER) and pesticide loading (PL). ER was defined as the ratio of the



encapsulated weight of imidacloprid to the theoretical weight of imidacloprid before encapsulation.

$$\text{ER}(\%) = \frac{\text{encapsulated weight of imidacloprid}}{\text{theoretical weight of imidacloprid}} \times 100\%$$

PL was defined as the ratio of the encapsulated weight of imidacloprid to the weight of imidacloprid microcapsules.

$$\text{PL}(\%) = \frac{\text{encapsulated weight of imidacloprid}}{\text{weight of imidacloprid microcapsules}} \times 100\%$$

Detailed procedures regarding the estimation of ER and PL were provided in the ESI.†

**2.3.2 Fourier transform infrared spectroscopy (FTIR).** The FTIR spectra of IMFs (IMSC, IMPDA and IMPU) were recorded by a Nicolet NEXUS-470 spectrometer (Thermo Fisher Scientific Inc., Madison, WI, USA) in transmission mode. The sample was prepared by mixing imidacloprid formulation of each type (~2 mg) with KBr and pressing under a hydraulic press (600 kg cm<sup>-2</sup>) to form a pellet for FTIR analysis. For each sample, 32 scans were performed with a spectral range of 400–4000 cm<sup>-1</sup> and a resolution of 4 cm<sup>-1</sup>.

**2.3.3 Thermogravimetric analysis (TGA).** The weight losses of IMFs (IMSC, IMPDA and IMPU) as well as PDA were determined by TGA with a Hitachi STA7300 TGA/DSC simultaneous thermal analyzer (Hitachi High-Technologies Co., Tokyo, Japan). The sample was heated from 20 to 900 °C at a ramp rate of 10 °C min<sup>-1</sup> in synthetic air (N<sub>2</sub> : O<sub>2</sub> = 4 : 1, v/v).

**2.3.4 Dynamic light scattering.** The size and size distribution of IMSC, IMPDA and IMPU were measured by dynamic light scattering. The instrument used was a Malvern Zetasizer (Model Nano-ZS90, Malvern Instruments, Inc., Houston, TX, USA). Before analysis, the suspension of each sample (5 wt%) was diluted 100 times with deionized water. All the measurements were conducted at 25 ± 0.1 °C with at least 3 runs on each sample suspension.

**2.3.5 Scanning electron microscopy (SEM).** The surface morphology of IMSC, IMPDA and IMPU was scanned under a Hitachi SU8010 scanning electron microscope (Hitachi High-Technologies Co., Tokyo, Japan) operating at an accelerating voltage of 15 kV. All samples were mounted on metal stubs and coated with gold–palladium by Denton Vacuum Desk II. In order to reduce the aggregation occurred under drying, the IMPU sample was prepared in a 0.5% dilute aqueous suspension containing 0.5% Triton X-100, and then painted on a silicon pellet with a brush before scanning.

**2.3.6 Water contact angle measurements.** The static water contact angles of IMFs (IMSC, IMPDA and IMPU) were determined by using the pendant drop method at 25 °C and 50% RH. The pellet of each IMF was prepared by pressing the formulation powder (50 mg) with a mold at room temperature under a load of 100 MPa for 5 min.<sup>32</sup> Then a water droplet of 2 μL was placed on the pellet and observed under an optical contact angle meter (Model SL 100B, Solon Information Technology Co., Ltd., Shanghai, China). Contact angle values for both sides

of the droplet were recorded. All samples were tested in at least four replicates.

**2.3.7 Viscosity test.** The viscosity of IMSC, IMPDA and IMPU were measured by a Rotational Viscometer (NDJ-1, Shanghai Changji Geological Instrument Co., Ltd., Shanghai, China). All measurements were conducted by using a 0# rotor at 25 ± 0.1 °C with at least 3 runs on each sample suspension.<sup>33</sup> Terminal velocity (m s<sup>-1</sup>) of sphere falling in a fluid was given by Stokes' law:

$$v = \frac{2(\rho_p - \rho_f)}{9\eta} gr^2 \quad (1)$$

where  $g$  is the gravitational acceleration (m s<sup>-2</sup>),  $\rho_p$  is the mass density of the particles (kg m<sup>-3</sup>),  $\rho_f$  is the mass density of the fluid (kg m<sup>-3</sup>),  $r$  is the radius of the spherical object (m), and  $\eta$  is the dynamic viscosity (Pa s).

## 2.4 Stability test

The stability of IMFs in solution after reaction was examined by natural sedimentation. The IMF suspension of each type (1 mL) was placed in a 2 mL clear glass vial with a PP screw cap and kept at room temperature. The suspensibility of IMFs was expressed as the percent of suspended IMFs over total IMFs after one month.<sup>33</sup>

$$\text{Suspensibility of IMFs}(\%) = \frac{m_{100} - m_{10}}{m_{100}} \times \frac{10}{9} \times 100\%$$

where  $m_{100}$  is the total weight of IMFs,  $m_{10}$  is the weight of sedimented IMFs in the bottom 10% volume of the suspension.

## 2.5 Release experiment for IMFs

The imidacloprid release experiment was carried out by injecting 100 μL IMF suspension (5 wt%) of each type (in triplicate) into a dialysis bag (molecular weights: 8000–14 000) and placing the bag in a PP centrifuge tube (50 mL) containing 50 mL deionized water as the release medium. The experiment was conducted under static condition at 25 °C until a steady state of imidacloprid release was achieved.

Imidacloprid released into water was measured by an ultraviolet-visible spectrophotometer (UNICO Shanghai Instrument Co., Ltd., Shanghai, China). Multiple samplings were taken at varied time intervals during the release experiment. A portion of sample solution (~3 mL) was transferred from the PP tube to a 1 cm optical path length quartz cell. A second quartz cell filled with pure water was used as a reference. The detection of imidacloprid in water was performed at a wavelength of 270 nm and a slit width of 5 nm. Imidacloprid standard solutions of six different concentrations in water were prepared to establish the calibration curve by plotting the absorbance against concentration. A good linear range was achieved between 1 μM and 50 μM ( $R^2 = 0.9993$ ). The limit of detection (LOD) of imidacloprid in water was determined to be 0.5 μM based on a signal-to-noise ratio of 3. Absorbance of each standard solution and sample solution was recorded 3 times, and the sample solution was returned to the PP tube after the measurement.



### 3. Results and discussion

#### 3.1 Characteristics of IMFs

FTIR analysis was employed to verify the encapsulation of imidacloprid. Fig. 1 shows the FT-IR spectra of IMSC, IMPDA and IMPU in the range of 400–4000  $\text{cm}^{-1}$ . Both IMPDA and IMPU spectra exhibit several characteristic bonds originating from the imidacloprid molecule. The two peaks at 3355  $\text{cm}^{-1}$  and 1280  $\text{cm}^{-1}$  are associated with the stretching of N–H and N–C of secondary amine, respectively. The three peaks at 1563  $\text{cm}^{-1}$ , 1480  $\text{cm}^{-1}$  and 1460  $\text{cm}^{-1}$  represent the stretching vibration of pyridine ring. A broader peak at 3355  $\text{cm}^{-1}$  was found for IMPDA and IMPU spectra than for IMSC spectrum, which should be caused by the overlapping of peaks for the adsorbed water, hydroxyl groups and amine groups in PDA.<sup>30,31</sup> In addition, the IMPU spectrum has two peaks at 2300  $\text{cm}^{-1}$  and 1640  $\text{cm}^{-1}$ , which are assigned to  $\text{N}=\text{C}=\text{O}$  stretching (unreacted isocyanate) and  $\text{C}=\text{O}$  stretching (amide:  $\text{NHCOO}$ ) in PU, respectively. Based on the FTIR results, both IMPDA and IMPU were successfully synthesized.

TGA was used to characterize the thermal stability of IMFs (Fig. 2). The TGA curve of IMSC shows only one-stage weight loss attributing to its decomposition. The curves of IMPDA and IMPU exhibit two weight loss stages due to the coating of IMSC with polymers. A new weight loss stage was found in the range of 300–600  $^{\circ}\text{C}$  which was assigned to the decomposition of

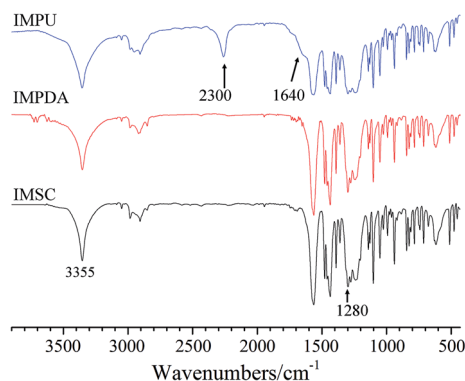


Fig. 1 FTIR spectra of IMSC, IMPDA and IMPU.

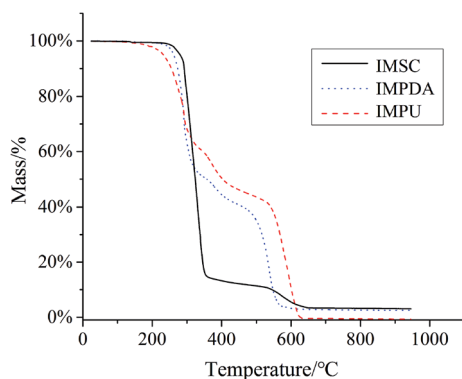


Fig. 2 TGA curves of IMSC, IMPDA and IMPU.

PDA.<sup>34</sup> Nevertheless, no obvious stage of PU decomposition was found in the IMPU curve. One reason could be that the thermal decomposition temperature of PU (prepared by the polymerization of IPDI) was closed to that of PDA ( $\sim 300$   $^{\circ}\text{C}$ ).<sup>35</sup> Another reason could be due to the strong interaction between PU and PDA, since the PU layer was synthesized on the PDA layer and bonded to the PDA layer.

#### 3.2 Size and size distribution

Fig. 3 shows the particle size and size distribution of IMSC, IMPDA and IMPU. The intensity-weighted mean diameters were  $474.5 \pm 136.8$  nm,  $970.7 \pm 238.2$  nm,  $1391 \pm 136.6$  nm for IMSC, IMPDA and IMPU, respectively. A broader size distribution was found for the encapsulated imidacloprid (IMPDA and IMPU) than for the non-encapsulated one (IMSC). Such phenomenon was attributed to two aspects: (a) part of the microcapsules were formed without the encapsulation of imidacloprid, resulting in smaller particles; and (b) adhesion of microcapsules occurred during the polymerization of PDA and PU, resulting in larger particles.

#### 3.3 Structure and morphology

The structure and morphology of IMFs are shown in the SEM images (Fig. 4). The particle sizes ranged mainly from 200 nm to 2  $\mu\text{m}$ , which was consistent with the results obtained by dynamic light scattering. The IMSC particles (Fig. 4a) exhibit a rod-like shape, which was caused by the breaking of IMTC particles (with a flake or thin needle crystal structure<sup>36</sup>) followed by the restructuring of the disrupted layers of IMTC during the wet grinding process. The smooth surface and regular shape of IMSC particles made them relatively easy to be encapsulated. The IMPDA particles (Fig. 4b) are more individually separated than the IMSC particles, since the PDA layer provides a barrier to isolate the IMSC particles and prevent them from aggregation. Partial aggregation was found for the IMPU particles (Fig. 4c), which could be caused by the adhesion among particles during the polymerization of IPDI with DETA.

#### 3.4 Hydrophobicity/hydrophilicity

The hydrophobicity/hydrophilicity of IMFs was related to the stability of IMF dispersion in solution, and can be evaluated with the static water contact angle. As shown in Fig. 5, the static water contact angles of IMSC, IMPDA and IMPU were  $58.35 \pm 1.45^{\circ}$ ,  $35.77 \pm 1.93^{\circ}$  and  $75.18 \pm 1.73^{\circ}$ , respectively. The contact angle was decreased when IMSC was coated with PDA, mainly attributing to the increased content of hydrophilic amine, imino and catechol groups at the IMPDA surface. The contact angle was increased after the PU layer was coated on IMPDA, since the hydrophilic functional groups (amine and imino groups) were reacted with IPDI (monomer of PU) and covered by PU. The change of contact angles among IMFs was another evidence for the successful encapsulation of imidacloprid.

#### 3.5 Stability of IMFs dispersion in solution

Dispersion stability is an important feature of pesticide formulations which is associated with the application efficacy.



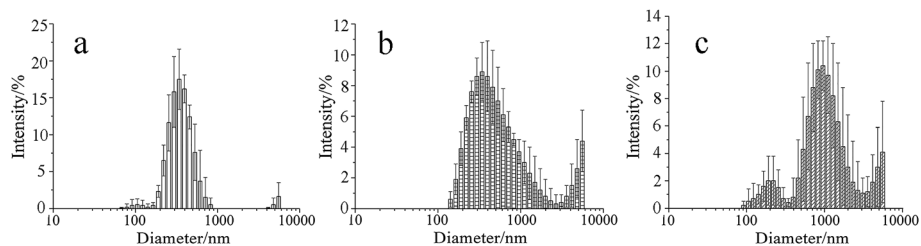


Fig. 3 Particle size and size distribution of (a) IMSC, (b) IMPDA and (c) IMPU.

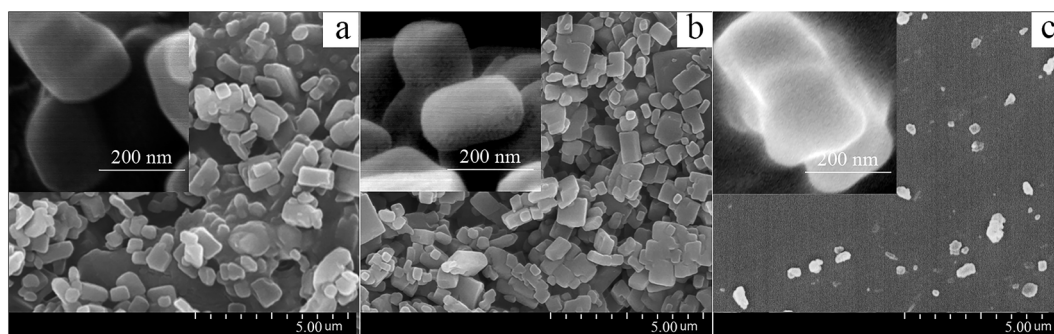


Fig. 4 SEM images of (a) IMSC, (b) IMPDA and (c) IMPU.

The stability of IMFs dispersion in the aqueous solution after reaction was examined; and the suspensibility values (after one month) were  $7.73 \pm 2.06\%$ ,  $69.01 \pm 1.21\%$  and  $90.60 \pm 0.33\%$  for IMSC, IMPDA and IMPU, respectively. The dispersion stability of IMFs followed the order of  $IMSC < IMPDA < IMPU$ . This trend was also observed in the natural sedimentation test (Fig. 6). The IMSC particles were stratified after 1 d and almost settled down after 7 d. The IMPDA suspension exhibited better

dispersion stability as the stratification and sedimentation occurred after 7 d and 14 d, respectively. The IMPU suspension had the most stable dispersion as no obvious stratification or sedimentation was observed within one month. IMSC was stratified quickly as the IMSC particles were easily aggregated due to their high surface energy, while hydrophilic microcapsule particles like IMPDA can repress the aggregation.<sup>32</sup> IMPU had the most stable dispersion possibly owing to the formation of low molecular weight amphiphilic molecules generated during the copolymerization of IPDI, dopamine, DETA and water, which in turn increased the microcapsule viscosity. The dynamic viscosities of IMFs were measured to be  $2.30 \pm 0.10$  mPa s,  $4.09 \pm 0.08$  mPa s and  $68.70 \pm 0.46$  mPa s for IMSC, IMPDA and IMPU, respectively. Assuming that the density of IMFs was about the same, the terminal velocity of microparticle settling was proportional to the square of particle radius and inverse proportional to the viscosity according to eqn (1). So, the terminal velocity in IMSC suspension was 3.5 times of that in IMPU suspension, and the terminal velocity in IMPDA suspension was almost 8 times of that in IMPU suspension.

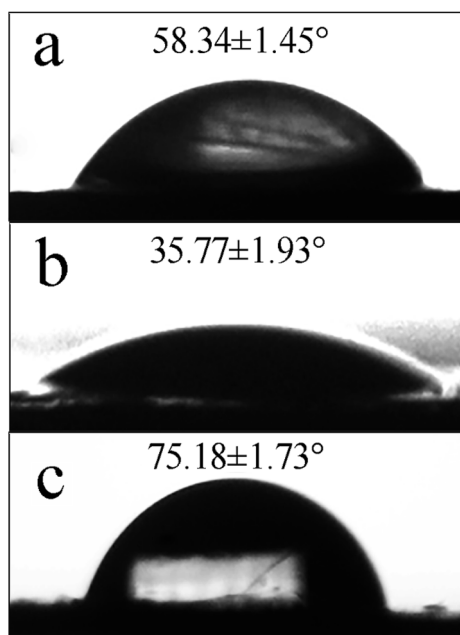


Fig. 5 Static water contact angles of (a) IMSC, (b) IMPDA and (c) IMPU.

### 3.6 Release of imidacloprid from IMFs

The ERs of IMPDA and IMPU were calculated to be  $39.94 \pm 3.07\%$  and  $47.28 \pm 0.87\%$ , respectively. The PLs were  $80.05 \pm 2.54\%$  for IMPDA and  $68.36 \pm 1.13\%$  for IMPU. These values were used to calculate the cumulative release rate in the sustained release test. The cumulative release curves of imidacloprid from the three types of IMFs are shown in Fig. 7. A rapid increase of the cumulative release rate was found at the beginning of the experiment, indicating a large amount of imidacloprid released from IMFs. Then the increase of the



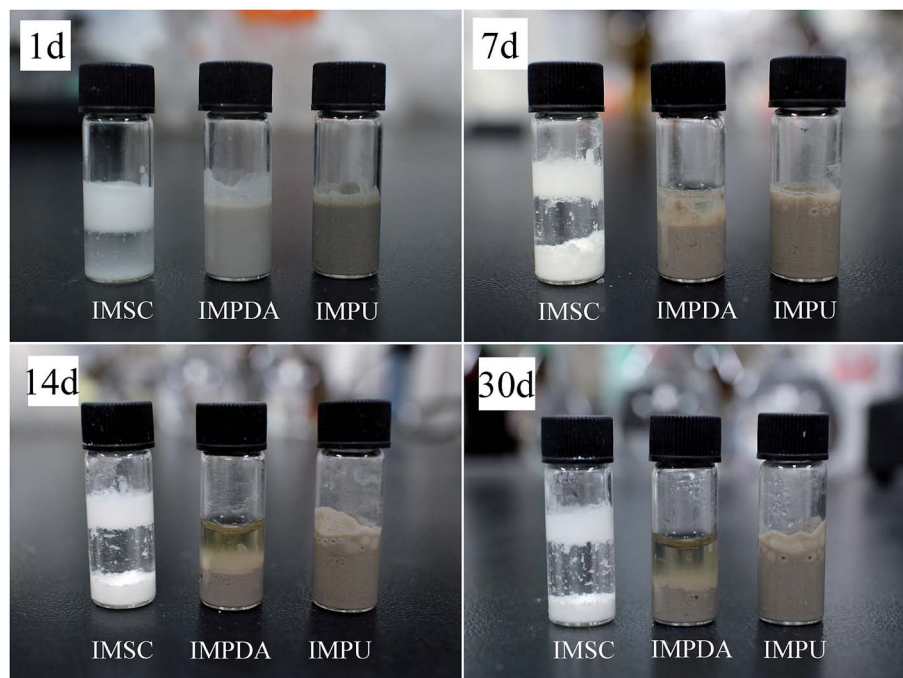


Fig. 6 Natural sedimentation of IMSC, IMPDA and IMPU in water with time.

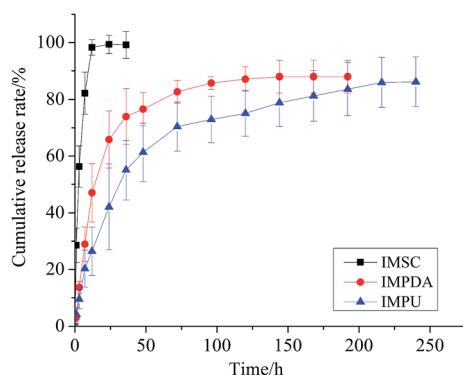


Fig. 7 Amount of imidacloprid released from IMFs into water as a function of time.

cumulative release rate was slowed down and finally reached a constant, indicating a steady state of imidacloprid release. The release of imidacloprid from IMSC was the most rapid as over 80% imidacloprid was dissolved in water in less than 7 h. The release of imidacloprid from IMPDA was slower and it took approximately 120 h to reach the steady state. PDA provided a superior barrier between the interior pesticide (imidacloprid) and the outer environment (water), and therefore delayed the imidacloprid release through a diffusion process in the polymer (PDA). The IMPU curve showed the slowest imidacloprid release; the steady state of release was achieved after 240 h. It was assumed that the addition of PU layer provided an extra barrier to further reduce the release of imidacloprid.

The release kinetics of imidacloprid from IMPDA and IMPU were expressed by the following equation:<sup>37</sup>

Table 1 Summary of parameters derived from eqn (2) for the imidacloprid release from IMPDA and IMPU

Sample	$k$	$n$	$R$
IMPDA	0.062	0.771	0.991
IMPU	0.045	0.703	0.997

$$\frac{M_t}{M_\infty} = kt^n \quad (2)$$

where  $M_t$  is the amount of imidacloprid released at time  $t$ ,  $M_\infty$  is the total amount of imidacloprid in microcapsules,  $k$  is a release constant, and  $n$  is a diffusional exponent which can be divided into three parts:  $n = 0.45$  for Fickian diffusion,  $0.45 < n < 0.85$  for anomalous transport, and  $n = 0.85$  for zero-order release caused by polymer erosion or relaxation.<sup>38</sup>

The experimental data obtained from the release experiment were fitted with the equation to solve the parameters associated with the release kinetics of imidacloprid, and the results are listed in Table 1. The release exponents ( $n$ ) of IMPDA and IMPU were 0.771 and 0.703, respectively. They were markedly exceeded the value of 0.45, revealing that the erosion of IMPDA and IMPU microcapsules was the dominant factor for the imidacloprid release.

## 4. Conclusions

The current study reported a novel imidacloprid microcapsule prepared by encapsulating imidacloprid with PDA followed by PU. No organic solvent or surfactant was used in the preparation process, which met the present demand of green process



and sustainability. The microcapsule exhibited excellent dispersion stability in the aqueous solution for a long period of time. In addition, the microcapsule was capable to release imidacloprid in a sustainable manner, allowing a much longer time to reach the steady state of release. A variety of pesticides can be encapsulated by PDA due to the oxidative self-polymerization of dopamine. Moreover, PDA can serve as a versatile platform for secondary surface modification, so that not only PU but also other polymers can be coated on PDA surface to achieve diverse functionalities.

## Acknowledgements

This work was supported by the Chinese National Scientific Foundation (21375146) and Ministry of Science and Technology of China (2016YFC0501205).

## Notes and references

- 1 P. Jeschke and R. Nauen, *Pest Manage. Sci.*, 2008, **64**, 1084–1098.
- 2 P. Jeschke, R. Nauen, M. Schindler and A. Elbert, *J. Agric. Food Chem.*, 2011, **59**, 2897–2908.
- 3 M. Tomizawa and J. E. Casida, *Annu. Rev. Pharmacol. Toxicol.*, 2005, **45**, 247–268.
- 4 A. Elbert, M. Haas, B. Springer, W. Thielert and R. Nauen, *Pest Manage. Sci.*, 2008, **64**, 1099–1105.
- 5 D. Goulson, *J. Appl. Ecol.*, 2013, **50**, 977–987.
- 6 C. A. Morrissey, P. Mineau, J. H. Devries, F. Sanchez-Bayo, M. Liess, M. C. Cavallaro and K. Liber, *Environ. Int.*, 2015, **74**, 291–303.
- 7 P. C. Lin, H. J. Lin, Y. Y. Liao, H. R. Guo and K. T. Chen, *Basic Clin. Pharmacol. Toxicol.*, 2013, **112**, 282–286.
- 8 T. S. Shim, S. H. Kim and S. M. Yang, *Part. Part. Syst. Charact.*, 2013, **30**, 9–45.
- 9 B. Hack, H. Egger, J. Uhlemann, M. Henriët, W. Wirth, A. W. P. Vermeer and D. G. Duff, *Chem. Ing. Tech.*, 2012, **84**, 223–234.
- 10 H. B. Scher, M. Rodson and K. S. Lee, *Pestic. Sci.*, 1998, **54**, 394–400.
- 11 A. P. Mihou, A. Michaelakis, F. D. Krokos, B. E. Mazomenos and E. A. Couladouros, *J. Appl. Entomol.*, 2007, **131**, 128–133.
- 12 K. Hirech, S. Payan, G. Carnelle, L. Brujes and J. Legrand, *Powder Technol.*, 2003, **130**, 324–330.
- 13 A. P. Rochmadi and W. Hasokowati, *Am. J. Appl. Sci.*, 2010, **7**, 39–45.
- 14 K. S. Mayya, A. Bhattacharyya and J. F. Argillier, *Polym. Int.*, 2003, **52**, 644–647.
- 15 T. Adak, J. Kumar, N. A. Shakil and S. Walia, *J. Environ. Sci. Health, Part B*, 2012, **47**, 217–225.
- 16 M. Li, Q. Huang and Y. Wu, *Pest Manage. Sci.*, 2011, **67**, 831–836.
- 17 M. Z. Kong, X. H. Shi, Y. C. Cao and C. R. Zhou, *J. Chem. Eng. Data*, 2008, **53**, 615–618.
- 18 F. Flores-Cespedes, C. Isabel Figueredo-Flores, I. Daza-Fernandez, F. Vidal-Pena, M. Villafranca-Sanchez and M. Fernandez-Perez, *J. Agric. Food Chem.*, 2012, **60**, 1042–1051.
- 19 R. Kanayama, *US Pat.*, 0182015-A1, 2009.
- 20 R. V. Jeanne and I. Rodriguez, *US Pat.*, 8680212-B2, 2014.
- 21 P. J. Mulqueen, A. Waller, J. L. Ramsay and G. W. Smith, *World Patent*, 072052-A2, 2007.
- 22 E. Olkowska, Z. Polkowska and J. Namiesnik, *Chem. Rev.*, 2011, **111**, 5667–5700.
- 23 A. F. Cirelli, C. Ojeda, M. J. L. Castro and M. Salgot, *Environ. Chem. Lett.*, 2008, **6**, 135–148.
- 24 H. Lee, S. M. Dellatore, W. M. Miller and P. B. Messersmith, *Science*, 2007, **318**, 426–430.
- 25 H. Lee, Y. Lee, A. R. Statz, J. Rho, T. G. Park and P. B. Messersmith, *Adv. Mater.*, 2008, **20**, 1619–1623.
- 26 L. Zhang, J. Shi, Z. Jiang, Y. Jiang, S. Qiao, J. Li, R. Wang, R. Meng, Y. Zhu and Y. Zheng, *Green Chem.*, 2011, **13**, 300–306.
- 27 L. Zhang, J. Shi, Z. Jiang, Y. Jiang, R. Meng, Y. Zhu, Y. Liang and Y. Zheng, *ACS Appl. Mater. Interfaces*, 2011, **3**, 597–605.
- 28 B. Yu, D. A. Wang, Q. Ye, F. Zhou and W. Liu, *Chem. Commun.*, 2009, 6789–6791.
- 29 H. Lee, J. Rho and P. B. Messersmith, *Adv. Mater.*, 2009, **21**, 431–434.
- 30 Z. Yang, Q. Tu, Y. Zhu, R. Luo, X. Li, Y. Xie, M. F. Maitz, J. Wang and N. Huang, *Adv. Healthcare Mater.*, 2012, **1**, 548–559.
- 31 M. Sureshkumar and C. K. Lee, *Carbohydr. Polym.*, 2011, **84**, 775–780.
- 32 L. Zhu, Y. Lu, Y. Wang, L. Zhang and W. Wang, *Appl. Surf. Sci.*, 2012, **258**, 5387–5393.
- 33 *CIPAC handbook. Volume F, Physico-chemical methods for technical and formulated pesticides. Collaborative International Pesticides Analytical Council*, ed. W. Dobrat and A. Martijn, 1994, pp. 393–395.
- 34 S. Zhang, Y. Zhang, G. Bi, J. Liu, Z. Wang, Q. Xu, H. Xu and X. Li, *J. Hazard. Mater.*, 2014, **270**, 27–34.
- 35 X. Qian, L. Song, B. Yu, W. Yang, B. Wang, Y. Hu and R. K. K. Yuen, *Chem. Eng. J.*, 2014, **236**, 233–241.
- 36 J. Zhao, M. Wang, B. Dong, Q. Feng and C. Xu, *Org. Process Res. Dev.*, 2013, **17**, 375–381.
- 37 R. W. Korsmeyer, R. Gurny, E. Doelker, P. Buri and N. A. Peppas, *Int. J. Pharm.*, 1983, **15**, 25–35.
- 38 S. Zuleger and B. C. Lippold, *Int. J. Pharm.*, 2001, **217**, 139–152.

